Appl Phys B (2009) 95: 597–601
DOI 10.1007/s00340-009-3447-6

Applied Physics B
Lasers and Optics

Ultra-narrow-band tunable laserline notch filter

C. Moser · F. Havermeyer

Received: 5 December 2008 / Revised version: 2 February 2009 / Published online: 3 March 2009

Abstract We report on an angularly tunable laserline notch filter from 760 to 785 nm with optical density of 5.7, 3 dB bandwidth of 9 cm^{-1} (0.55 nm) and greater than 80% transmission. The notch filter is a single element composed of six bonded slanted reflective holographic gratings in glass.

PACS 42.40.Eq · 42.40.My · 42.40.Pa

1 Introduction

A laserline notch rejection filter is an essential component in Raman instruments. The purpose of the notch filter is to greatly attenuate the backscattered light from the laser illuminating a sample under test, while letting the faint Raman spectrally shifted signature pass through. Two non-dispersive filter technologies are currently used for notch filters: holographic and thin film. Commercial holographic notch filter technology uses holographic recording in a thin film of dichromated gelatin to produce a notch filter with 3 dB bandwidth of 350 cm^{-1} at 780 nm and optical density of 6 [1]. Commercial thin film technology uses deposition of many dielectric layers to obtain a 3 dB bandwidth of approximately 600 cm^{-1} and optical density of 6 [2]. Both technologies provide a compact size, notch filter element with a 10 mm aperture diameter and several millimeters thickness. However, both notch filter technologies are limited to observing Raman spectral shift above approximately 350 cm^{-1}.

The Raman signal in the low frequency shift region, i.e. near the frequency of the excitation laser, contains critical information about the molecular structure. For example, carbon nanotubes exhibit vibration modes in the range of 150 to 200 cm^{-1} depending on their size [3, 4]. Relaxation in liquids, solutions and biological samples exhibit Raman shift, in the range between 0 and 400 cm^{-1} [5].

The state-of-the–art technology utilized to observe Raman signals close to the laser excitation is based on cascading dispersive spectrometers [6]. The cascaded spectrometers are bulky (∼1 m^2), expensive (∼100 K) and of moderate transmission (∼50%).

In this letter we demonstrate a non-dispersive holographic notch filter technology capable of observing the Raman signal near the excitation wavelength (9 cm^{-1}). The novelty of the approach is the compactness of the notch filter (same size as a standard thin film/holographic notch filter) realized by bonding individual notch filters without creating spurious multiple diffractions. Such ultra-narrow-band laserline notch filters can thus be used in standard compact Raman instruments and help bring high-end research to a greater number of users.

2 Narrow-band volume holographic notch filters in glass

Reflective volume holographic filters (VHGs) with millimeters thickness are rejection notch filters producing 3 dB bandwidth of the order of 10 cm^{-1} [7]. VHGs produced in a glass material are now commercially available and show both long lifetime, high efficiency and excellent transmission in the red and near infrared. Large area (30 × 30 mm) reflective VHGs are restricted to the millimeter range thickness [8] due to the material absorption. The optical density achievable is of the order of 1 (i.e. ∼90% efficiency) with

C. Moser (✉) · F. Havermeyer
Ondax, Inc., 850 E. Duarte Road, Monrovia, CA 91016, USA
e-mail: moser@ondax.com

thickness of 1 mm and transmission of 97 to 98% away from the notch in the near infrared.

By carefully individually aligning a cascade of VHGs, others have shown that the optical density can be added: a cascade of 4 VHGs, each exhibiting an optical density of one yields a compounded notch filter with an optical density of 4. Commercial instruments comprising individual alignment fixtures for each VHG exhibit an optical density ranging from 4 to 6 with bandwidth of 10 cm^{-1} [9]. However, the footprint of such an approach is larger (100 cm^3 versus 6.5 cm^3) and requires individual alignment of each VHG.

Below we show a method to align and bond a cascade of VHGs so as to overcome the limitations outlined above.

3 Alignment and bonding of multiple reflective VHGs

The notch wavelength λ_B of a reflective VHG is characterized by the grating period Λ and the angle of incidence Θ of the collimated illumination on the grating planes:

$$\lambda_B = \lambda_0 \cdot \cos(\Theta), \tag{1}$$

where $\lambda_0 = 2 \cdot n \cdot \Lambda$ is the anti-parallel diffraction wavelength and where n is the index of refraction.

Identical reflection VHGs, i.e. VHGs characterized by the same grating period, Λ, and incidence angle, Θ, cannot simply be stacked since the diffracted beams will fulfill the Bragg condition for other VHGs in the stack. Double diffraction on individual VHGs will cause interference effects and prevent the optical density values to be simply added.

However, by varying the grating slant (the angle between the grating vector and the VHG surface normal) and the grating spacing, Λ, of each individual VHG in such a way that the same wavelength fulfills the Bragg condition for each VHG, the diffracted light from subsequent VHGs does not full fill the Bragg condition on any other grating. Figure 1 illustrates the construction for a stack of two VHGs. The direction of diffraction for the first and second diffracted beam $\vec{k}_{d1}$ and $\vec{k}_{d2}$ are at an angle such that $\vec{k}_{d2}$ propagates through the first VHG without re-diffracting.

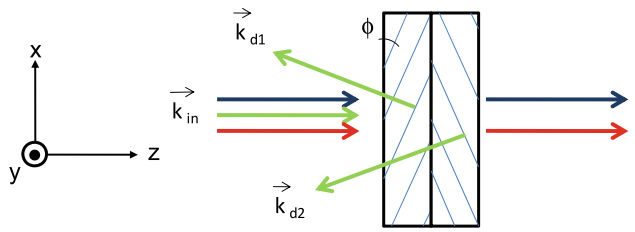

Fig. 1 Schematic of a stack of two narrow-band reflection VHGs. Collimated illumination is incident on both VHGs at the same angle, but different grating slant angles ϕ diffract the light into different directions $\vec{k}_{d1}$ and $\vec{k}_{d2}$. Individual grating spacings Λ and slant angles ϕ are chosen such that at each VHG, the same wavelength fulfills the Bragg condition

Below, we address two key challenges. The first challenge is to design the VHGs so that the entire assembly of the stacked VHGs is wavelength tunable by rotation while keeping the bandwidth and optical density constant. The second challenge is to align the successive VHGs in the stack such that their notch wavelength overlaps to maximize the optical density.

3.1 VHG design and stack alignment

For the following analysis, we will assume that the collimated incident beam wave vector outside the material is parallel to the z-axis (see Fig. 1): $\vec{k}_{\text{air}} = k_{\text{air}}\vec{e}_z$. The first and last VHG of the stack is surrounded by air. We assume no Fresnel losses between bonded VHGs. We will allow for a grating slant ϕ (angle between grating vector and surface normal) only in the x–z-plane. We assume that the illumination is well collimated and of single frequency. The laser wavelength is chosen slightly below the normal incidence wavelength of each VHG in the stack.

Following the illustration in Fig. 2, the first VHG is positioned with its grating vector $\vec{K}$ in the x–z-plane and rotated around the x-axis to fulfill the Bragg condition according to (1). The facet normal of the first VHG defines the incidence angle Θ_M of the entire stack with respect to the collimated illumination direction $\vec{k}_{\text{air}}$. The orientations of the facet normals of subsequent VHGs with respect to the incident beam, i.e. Θ_M are collinear with each other since we assume the VHG in the stack are in mechanical contact.

For the subsequent VHGs, fine wavelength tuning is achieved by rotating the VHG around its surface normal, the only degree of freedom left, by an angle ω.

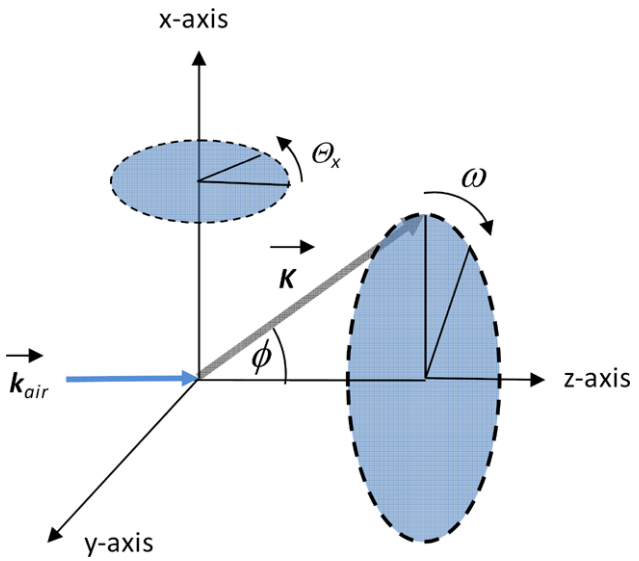

Fig. 2 Fine alignment for each VHG: orientation of the incident beam wave vector $\vec{k}_{\text{air}}$ is chosen along the z-axis. Each VHG, characterized by its grating vector $\vec{K}$, is first rotated by an angle Θ_x around the x-axis and then by an angle ω around the z-axis

Using Snell's law, the incident beam wave vector in the material is

$$\vec{k} = k \begin{pmatrix} 0 \\ -\sin(\Theta_x - \Theta_M) \\ \cos(\Theta_x - \Theta_M) \end{pmatrix}$$

$$\text{with } \Theta_M = \operatorname{asin}\big(\sin(\Theta_x)/n\big), \tag{2}$$

where $\Theta_x - \Theta_M$ is the angle between z-axis and $\vec{k}$, and Θ_M is the angle between surface normal and $\vec{k}$ measured inside the medium. After rotation of the VHG around the x-axis by an angle Θ_x, and around the surface normal by angle ω, the VHG's grating vector $\vec{K}$ is

$$\vec{K} = K \begin{pmatrix} \cos(\omega)\sin(\phi) \\ \cos(\Theta_x)\sin(\omega)\sin(\phi) - \sin(\Theta_x)\cos(\phi) \\ \sin(\Theta_x)\sin(\omega)\sin(\phi) + \cos(\Theta_x)\cos(\phi) \end{pmatrix}. \tag{3}$$

Using $\cos(\Theta) = \vec{k}\cdot\vec{K}/(kK)$ and (3), we find the notch wavelength λ_B as a function of the angles ω and Θ_M:

$$\lambda_B = \lambda_0 \cos(\phi)\big(\cos(\Theta_M) + \sin(\Theta_M)\sin(\omega)\tan(\phi)\big). \tag{4}$$

From (4), we observe that individual VHGs can be Bragg-matched to the required notch wavelength by adjusting the rotation angles ω_i for each grating $i = 2, \ldots, N$. The fine wavelength tuning is only possible when $\Theta_M, \phi_i > 0$.

As an example of a six VHG stack, the diffraction diagram in K-space is illustrated in Fig. 3. Each VHG has its own distinct slant angle and grating period.

A typical angular selectivity curve for an individual VHG is given in Fig. 4. The angular 3 dB bandwidth is 0.4 degrees. The slant angle of each VHG is chosen such that the diffracted beams do not satisfy the Bragg condition for all other VHGs. From the measurement shown in Fig. 4, a value of at least 1 degree for the slant angle has been selected to satisfy that condition.

For the experiment, we prepared six individual reflection VHGs with thickness of 1.6 mm and diffraction efficiencies near 90% (corresponding to optical density near unity). Anti-parallel diffraction wavelength and slant angles are given in Table 1. Each of the successive five VHGs is brought into direct mechanical contact to the previous VHG. After alignment individual gratings are secured to the stack by an index matching epoxy. This procedure ensures that the internal incident angle Θ_M is the same for every grating in the stack. Only the rotation angle ω_i is used to fine-tune the notch wavelength.

The laser used for the alignment is a wavelength locked semiconductor laser diode at 785.35 nm, which is subsequently ASE filtered by a slanted reflection VHG (Ondax, Inc, laser TO-785-PLR80 with one ASE filter 114-80008-001). Grating #1 is aligned for Bragg diffraction with $\omega_1 \approx 0$ and $\Theta_M = 2.7$ deg.

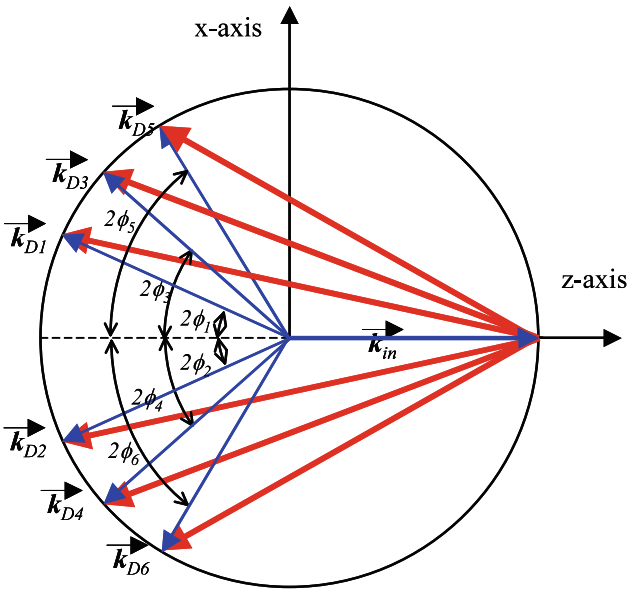

Fig. 3 Schematic wave-vector diagram for a stack of six gratings. The drawing omits all wave-vector components in the y-direction for clarity. The single input wave vector $\vec{k}_{\text{in}}$ fulfills the Bragg condition for every grating. The diffracted beams $\vec{k}_{Di}$ for $i = 1, \ldots, 6$, which are at an angle $2\phi_i$ to the z-axis, do not satisfy the Bragg condition of all other gratings

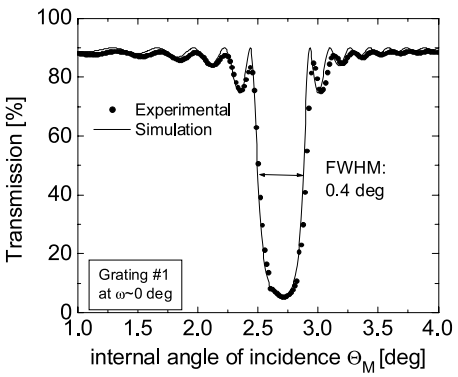

Fig. 4 Typical angular selectivity at the alignment wavelength. The angular FWHM is approximately 0.4 deg FWHM inside the glass. Notice that the grating surfaces are not AR coated resulting in a loss of ~8% due to reflection

Now, let us determine what happens when the stack of bonded VHGs is wavelength tuned. Wavelength tuning is performed by varying the incident angle from the initial alignment angle Θ_M to a new incident angle $\Theta_M + \Delta\Theta_M$. For all VHGs in the stack, the new notch wavelength will vary according to (4) and the difference in wavelength between any two gratings can be computed to be

$$\Delta\lambda = \big(\lambda_{0,1}\cos(\phi_1) - \lambda_{0,2}\cos(\phi_2)\big)\frac{\sin(\Delta\Theta_M)}{\sin(\Theta_M)}. \tag{5}$$

The wavelength shift between any two gratings does not depend on the rotation terms ω_i. This is due to the constraint

Table 1 Measured anti-parallel diffraction wavelength $\lambda_{0,i}$, slant angle ϕ_i and peak diffraction efficiency η for six gratings. Also given is the normal incidence wavelength $\lambda_{0,i}\cos(\phi_i)$, which determines the tuning range of the final stack. The average normal incidence wavelength $\lambda_{0,i}\cos(\phi_i)$ is (785.84 ± 0.069) nm

VHG #	$\lambda_{0,i}$ [nm]	ϕ_i [deg]	$\lambda_{0,i}\cos(\phi_i)$ [nm]	η [%]
1	785.96	+0.94	785.85	93
2	786.04	−1.02	785.92	92
3	786.10	+1.50	785.83	93
4	786.18	−1.50	785.91	91
5	786.32	+2.02	785.83	92
6	786.20	−1.99	785.73	91

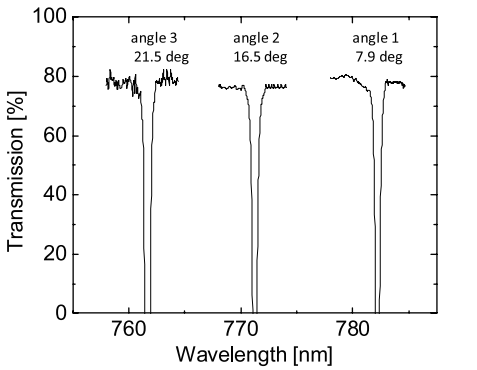

	FWHM [nm]/[cm-1]	Bandwidth @ 90% transmission [nm]/ [cm-1]
Angle 1	0.50 / 8.17	1.06 / 17.32
Angle 2	0.55 / 9.24	1.10 / 18.49
Angle 3	0.64 / 11.03	1.18 / 20.85

Fig. 5 Transmission curve shown for three angles (in air) of a stack of six VHGs bonded together forming a notch filter spectrally tuned by rotating the filter around the x-axis. The measured broadening of the bandwidth at the largest angle is equal to 0.14 nm, in good agreement with the expected broadening of 0.25 nm

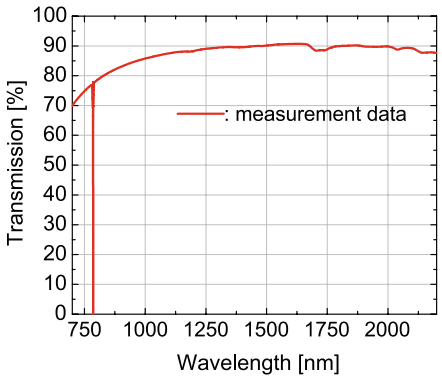

Fig. 6 Spectral transmission of the stack of six bonded VHGs. Measurement is taken with a CARY 500 spectrometer with a 2 nm resolution and non-collimated light

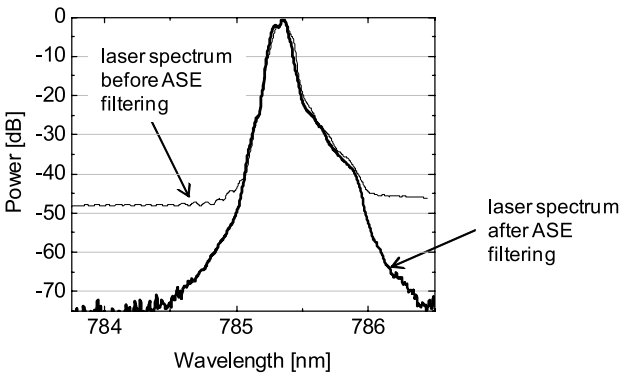

Fig. 7 Wavelength spectrum of the wavelength locked laser diode showing amplified spontaneous emission (ASE) that results in a continuous background of light with intensities up to 50 dB below peak intensity. Filtering the output beam by two slanted reflection VHGs effectively removes the background

that at the alignment angle Θ_M of the stack, the wavelength shift $\Delta\lambda$ is equal to zero.

Table 1 gives a standard deviation of 0.069 nm for the quantity $(\lambda_{0,i}\cos(\phi_i) - \lambda_{0,j}\cos(\phi_j))$.

The stack of six VHGs was aligned at a value for Θ_M of 2.7 degrees and tuned by $\Delta\Theta_M$ of 11.4 degrees (these are values inside the material of index $n = 1.5$). According to (5), we expect to observe a broadening of the overall bandwidth by 0.29 nm. The experimental result is shown in Fig. 5. As expected, the six-stack notch filter maintains a single transmission notch at all tuning angles. The measured spectral bandwidth broadening is half the computed value (0.14 versus 0.29 nm).

Light transmission of the six-stack wavelength notch filter is measured by a CARY 500 spectrometer. The transmission measurement in Fig. 6 shows that the 9.6 mm thick filter stack transmit greater than 80% of the incident light outside the notch. The first and last VHG facets are without anti-reflection (AR) coatings. An additional 8% transmission could be gained by adding an AR coating to the outside facet of the first and last VHG in the stack.

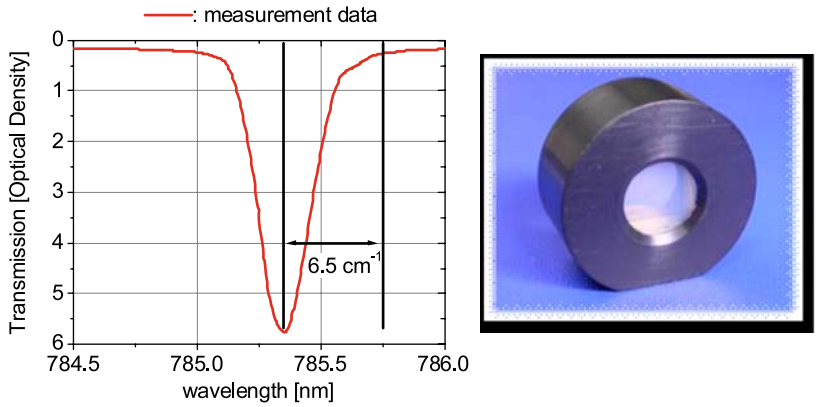

Fig. 8 Spectrum of the six-stack laserline notch filter showing an optical density of 5.7. A picture of the filter is shown on the *right*. The aperture of the filter is 9.3 mm and the holder has a diameter of 25.4 mm (1 inch)

The optical density of the fabricated stack is measured with the same ASE filtered laser source used above for the alignment. Figure 7 shows the spectrum of the unfiltered and filtered laser diode measured with an ANDO double spectrometer with 0.05 nm resolution. We observe that the ASE of the original laser diode is drastically reduced. The spectrometer distorts and broadens the actual ASE filtered spectrum due to stray light inside the spectrometer.

The ASE filtered collimated light beam of dimension 1 mm × 2 mm is incident on the laserline notch filter, which is mounted on a rotation stage. The transmitted light is coupled into a 100 micrometer fiber. The other end of the fiber illuminates a detector. This detection scheme is used to reduce stray light into the detector. The transmitted power is monitored while the notch filter is rotated. The measured angular selectivity curve is then converted into a spectral transmission curve. Figure 8 shows the spectral transmission curve of the laserline notch filter displayed in logarithmic scale (optical density).

4 Summary and conclusion

We have shown a method to construct a multi-stack laserline notch filter with a 3 dB bandwidth of 9 cm^{-1} (0.55 nm) and optical density of 5.7 that is maintained upon wavelength tuning. We have also developed a wavelength locked ASE filtered semi-conductor source near 785 nm as a compact single frequency excitation source. The ASE filtered laser source is necessary to observe the low frequency Raman signal.

This ultra-narrow-band laserline notch filter has dimensions similar to standard Raman notch filters (9.3 mm aperture mounted into a 25.4 mm holder). The footprint compatibility of this novel high performance filter with standard compact Raman instruments is expected to help bring the high-end research of low-frequency Raman analysis to a greater number of users.

References

1. Kaiser Optical System datasheet, http://www.kosi.com/Holographic_Filters/standard.php
2. Semrock datasheet, http://www.semrock.com/Catalog/Category.aspx?CategoryID=75
3. M.N. Iliev, A.P. Litvinchuk, Chem. Phys. Lett. **316**(3–4), 217–221 (2000)
4. C.Y. Wang, C.Q. Ru, A. Miuduchowski, J. Appl. Phys. **97**, 024310 (2005)
5. Y. Amo, Y. Inadachi, Y. Tominaga, J. Chem. Phys. **119**(20), 10801–10805 (2003)
6. R. Schaeffer, O. Rohm, D. Koulikov, A. O'Grady, Spectrosc. Mag. 33–34 (March 2006)
7. V. Leyva, G.A. Rakuljic, B. O'Conner, Opt. Lett. **18**, 459 (1993)
8. C. Moser, G. Steckman, Photonics Spectra 82–86 (June 2005)
9. Photon Etc. datasheet, http://www.photonetc.com/media/pdf/Top%20Notch%20Filter%20datasheet.pdf